

CHAPTER IV

APPLICATION: $^{16}\text{O} - ^{16}\text{O}$ ELASTIC
SCATTERING BY SEMICLASSICAL METHOD

IV. 1. Introduction

Semiclassical methods have already been used extensively in the study of heavy ion collision. The methods have been found quite useful in determining various qualitative aspects of the collision phenomena. However, the accuracy of the semiclassical results in most of the cases are not satisfactory. We intend to study here the applicability as well as the accuracy of the generalized Miller-Good method by considering a realistic problem e.g. $^{16}\text{O} - ^{16}\text{O}$ elastic scattering. We have considered this problem in two parts. First, we have applied the real Miller-Good method. Since the absorptive part of the nuclear potential cannot be neglected, we had to make use of a perturbative approach for the imaginary part of the potential. Thus the turning point is determined by the real part of the potential and the phase integral is taken along a real trajectory. The imaginary part only supplied a damping factor to each of the partial waves. This approximation is good if the imaginary part is small. If the Miller-Good method is found suitable for a realistic problem, it may eliminate in some cases a lengthy direct numerical calculation, particularly if the accuracy demanded is not too high. In this context, we have also applied the complex Miller-Good method to study the same problem.

In the actual calculation, we have made a departure from the usual trend in connection with the choice of the coulomb part of the potential. In the study of heavy ion collision, the coulomb part of the potential is usually

taken in an approximate way. The potential chosen is given by either (a) that between a point charge and a sphere of uniform density or (b) that between two uniformly charged spheres of appropriate radii. The approximation appears to be a good one when the nuclei are heavy and have Fermi type of charge distributions. However, it is not obvious why this approximation should be valid for light nuclei like ^{12}C , ^{16}O etc. which have been used as projectiles for many experiments. These p-shell nuclei have a modified harmonic well type of charge distribution, which cannot be represented well by a uniform distribution. It is well-known that the elastic scattering of heavy ions depend more crucially on the real part of the potential around a critical distance $R \sim 1.5 (A_1^{\frac{1}{3}} + A_2^{\frac{1}{3}})$ fm. Thus the elastic scattering normally places a very weak constraint on the detailed structure of the potential. However, considering also phenomena like the fusion and the nucleon transfer reactions one can determine the potential more accurately. The choice of the correct coulomb potential will, therefore, be more useful when the entire range of experimental results (elastic scattering, fusion and transfer reactions) are sought to be explained with the same set of potential parameters. It seems, therefore, worthwhile to see if the inaccuracy in the charge distribution chosen is reflected in the measurable quantities, particularly in the scattering cross-sections. With this view in mind we have considered here two cases: (A) the case of two uniformly charged spheres of radii $\sqrt{5/3} R_{\text{r.m.s.}}$ and (B) the case

of the two diffuse charge distributions of the modified harmonic well type. The coulomb potential in both the cases can be calculated analytically by making use of the convolution theorem of Fourier transforms. The nuclear potential between the nuclei was assumed to be given by a complex Woods-Saxon function. The phase shifts and the scattering cross-sections for a pair of p-shell nuclei ($^{16}\text{O} - ^{16}\text{O}$) were then calculated by the generalized semiclassical method. The results indicate some difference in phase shifts and in cross-sections in the cases (A) and (B). It may, therefore, be worthwhile to work with the correct charge distribution instead of the approximate distribution(A), which is commonly used in heavy ion codes¹.

The presentation of the material is as follows. In section IV.2., we have given the expressions for the coulomb potential between two colliding nuclei. The semiclassical method has been discussed in section IV.3. The calculated results are presented and analysed in section IV.4. In the next section, we shall study the $^{16}\text{O} - ^{16}\text{O}$ elastic scattering by the complex Miller-Good (CMG) method. The results will be compared with other results, theoretical and experimental. Our conclusions are also summarized there.

IV.2. The coulomb potential

To calculate the coulomb potential between the colliding nuclei we make use of the following results:

If the charge form factors of the nuclei A and B are $f_1(\vec{q})$ and $f_2(\vec{q})$, \vec{q} being the momentum

transferred, the potential between them in momentum space is given by

$$V(\vec{q}) = \frac{4\pi}{q^2} z_1 z_2 e^2 f_1(\vec{q}) f_2(\vec{q}) \quad \dots(4.1)$$

The expression (4.1) follows easily from the convolution theorem of Fourier transforms. The potential in the coordinate space is given by

$$V_c(\vec{r}) = \frac{1}{(2\pi)^3} \int d^3q e^{-i\vec{q}\cdot\vec{r}} v(\vec{q}), \quad \dots(4.2)$$

and if the charge distribution is spherically symmetric,

$$V_c(r) = \frac{2 z_1 z_2 e^2}{\pi r} \int_0^\infty dq \left(\frac{\sin qr}{q} \right) f_1(q) f_2(q). \quad \dots(4.3)$$

We shall consider two special cases:

Case I: When the colliding nuclei have charge distributions given by the generalized shell model (GSM).

It has been generally accepted² that for nuclei with an incomplete 1p shell, the charge distribution is given by

$$\rho(r) = \frac{2}{\pi^{3/2}} \frac{1}{a_0^3 (2 + 3\alpha)} \left(1 + \alpha \frac{r^2}{a_0^2} \right) \exp(-r^2/a_0^2), \quad \dots(4.4)$$

where

$$a_0 = \left(\frac{\hbar^2}{M\epsilon} \right)^{\frac{1}{2}}, \quad \dots(4.5)$$

ϵ being the energy interval between two consecutive levels of the harmonic oscillator. The root mean square radius (a) of the distribution is given by

$$a = a_0 \sqrt{\frac{3(2+5\alpha)}{2(2+3\alpha)}} \quad \dots(4.6)$$

with

$$\alpha = \frac{1}{3} (Z-2) \quad \dots(4.7)$$

The form factor for the distribution (4.4) can be easily evaluated and is seen to be given by

$$F(q) = \left[1 - \left(\frac{\alpha q^2 a_0^2}{2(2+3\alpha)} \right) \right] \exp \left(-\frac{q^2 a_0^2}{4} \right) \quad \dots(4.8)$$

Assuming that both the nuclei have charge distributions of the type (4.4), we have calculated the coulomb potential exactly by using the relation (4.3). This can be written as

$$V_c(r) = Z_1 Z_2 e^2 \left[\frac{1}{r} \operatorname{Erf} \left(\frac{r}{2B} \right) + (\beta + \gamma r^2) e^{-r^2/4B^2} \right] \quad \dots(4.9)$$

where

$$\beta = \left[3 A_1 A_2 - 2(A_1 + A_2) B^2 \right] / 4B^5 \sqrt{\pi} \quad \dots(4.10)$$

$$\gamma = - A_1 A_2 / 8B^7 \sqrt{\pi} \quad \dots(4.11)$$

$$B^2 = B_1^2 + B_2^2 \quad \dots(4.12)$$

with

$$A_i = \alpha_i a_{oi}^2 / [2 + (2 + 3\alpha_i)] \quad \dots(4.13)$$

$$B_i^2 = a_{oi}^2 / 4 \quad , \quad \dots(4.14)$$

the suffix i ($i = 1, 2$) referring to the i -th nuclei.

Case II: When the colliding nuclei have uniform charge distributions:

The charge distribution here is given by

$$\begin{aligned} \rho(r) &= \rho_0 & \text{for } r < R \\ &= 0 & \text{for } r > R \end{aligned} \quad \dots(4.15)$$

R being the radius of the charged sphere. The corresponding form factor is given by

$$f(q) = \frac{1}{q^3 R^3} \left[\sin qR - qR \cos qR \right] \quad \dots(4.16)$$

From (4.3) and (4.16) one gets³

(i) for $r > R_1 + R_2$,

$$V_c(r) = \frac{Z_1 Z_2 e^2}{r} \quad \dots(4.17)$$

(ii) for $r < R_1 - R_2$,

$$V_c(r) = \frac{Z_1 Z_2 e^2}{R_1} \left[\frac{3}{2} - \frac{1}{2} \frac{r^2}{R_1^2} - \frac{3}{10} \frac{R_2^2}{R_1^2} \right] \quad \dots(4.18)$$

(iii) for $R_1 - R_2 < r < R_1 + R_2$,

$$V_c(r) = Z_1 Z_2 e^2 \left[\frac{1}{r} + \frac{1}{160 r (p_1 p_2)^3} \sum_{j=0}^6 C_j (p_1 + p_2)^j \right] \quad \dots(4.19)$$

where

$$p_i = \frac{R_i}{r}, \quad i = 1, 2 \quad \dots(4.20)$$

and

$$\begin{aligned}
 C_0 &= -30 P_1 P_2 - 1 \\
 C_1 &= 120 P_1 P_2 \\
 C_2 &= 15 - 180 P_1 P_2 \\
 C_3 &= 120 P_1 P_2 - 40 \\
 C_4 &= 45 - 30 P_1 P_2 \\
 C_5 &= -24 \\
 C_6 &= 5 .
 \end{aligned}
 \tag{4.21}$$

For two identical nuclei, the potential can be written in a simpler form, viz:

$$\begin{aligned}
 V_c(r) &= \frac{Z^2 e^2}{r} \left\{ 1 + \frac{1}{160 R^6} (30 r^4 R^2 - r^6 - 80 R^3 r^3 \right. \\
 &\quad \left. + 192 R^5 r - 160 R^6) \right\} , \\
 &\quad r < 2R \\
 &= \frac{Z^2 e^2}{r} , \quad r > 2R
 \end{aligned}
 \tag{4.22}$$

We shall do the calculations here with both the potentials (Case I) and (Case II). The nuclear part of the potential for $^{16}\text{O} - ^{16}\text{O}$ will be taken to be a complex optical model potential, as chosen by Maher et al⁴, viz;

$$V_N(r) = \frac{-(V_0 + i W_0)}{1 + \text{Exp}\left(\frac{r - R_0}{a_0}\right)} \quad \dots(4.23)$$

with W_0 depending on the collision energy.

IV.3. Semiclassical phase shifts and cross-sections

We shall consider here a perturbative method for treating the complex optical potential, assuming that the imaginary part of the potential is small. Thus instead of working with the wave vector

$$K(r) = \left[K^2 - \frac{2\mu}{\hbar^2} (V_R + i V_I) - \frac{L(L+1)}{r^2} \right]^{\frac{1}{2}}, \quad \dots(4.24)$$

we expand and keep terms upto first order in V_I . The contribution of the imaginary part in this approximation is contained in a damping factor $e^{-2S(L)}$ for each partial wave of angular momentum L , where

$$S(L) = \frac{2\mu}{\hbar^2} \int_{r_0}^{\infty} \frac{V_I dr}{2 \left[K^2 - \frac{2\mu}{\hbar^2} V_R - \frac{L(L+1)}{r^2} \right]^{\frac{1}{2}}} \quad \dots(4.25)$$

Apart from this damping factor, the problem is now that of a real potential. Consequently, the turning point and

the trajectory are both real and the generalized semiclassical method can be applied to this problem in a straightforward manner. The parameters chosen for the Woods-Saxon potential⁴ for $^{16}_0 - ^{16}_0$ scattering indicate that W_0 is indeed much smaller than V_0 , at least upto about $E_{cm} = 50$ Mev. Thus, the approximation made above may be acceptable.

The details of the semiclassical method have already been given in chapter II. The method has been found to give accurate results even at low energies, where the conventional JWKB method is inaccurate. We shall consider only terms of lowest order in \hbar^2 . We have chosen as the model equation, the radial equation for scattering from a point charge with the same Sommerfeld parameter,

$$n = \frac{2\mu}{\hbar^2} \frac{Z_1 Z_2 e^2}{2K}, \quad \dots(4.26)$$

where $K^2 \hbar^2 / 2\mu$ is the C.M. energy. To obtain an expression for the phase shifts, we first write the radial equation for the problem as

$$\frac{d^2 R_L(y)}{dy^2} + \frac{t_1(y)}{\hbar^2} R_L(y) = 0, \quad \dots(4.27)$$

with

$$\frac{1}{\hbar^2} t_1(y) = 1 - \frac{L(L+1)}{y^2} - \frac{2\mu}{\hbar^2 K^2} (V_N + V_C), \quad \dots(4.28)$$

where $y = Kr$ and $V_N(y)$ and $V_C(y)$ are the nuclear and coulomb part of the potential respectively. The model equation is also written as

$$\frac{d^2 R_L^0(s)}{ds^2} + \frac{t_2(s)}{\hbar^2} R_L^0(s) = 0, \quad \dots(4.29)$$

with

$$\frac{1}{\hbar^2} t_2(s) = 1 - \frac{2n}{s} - \frac{L(L+1)}{s^2}. \quad \dots(4.30)$$

Let us now introduce Langer's substitution

$$y = e^x,$$

$$R_L(y) = e^{x/2} G_L(x) \quad \dots(4.31)$$

to obtain the transformed radial equation for the problem as

$$\frac{d^2 G_L(x)}{dx^2} + \frac{q_1(x)}{\hbar^2} G_L(x) = 0, \quad \dots(4.32)$$

where

$$\frac{1}{\hbar^2} q_1(x) = e^{2x} \left[1 - \frac{2\mu}{\hbar^2 K^2} V_C^1(x) - \frac{2\mu}{\hbar^2 K^2} V_N^1(x) \right] - \left(L + \frac{1}{2} \right)^2 \quad \dots(4.33)$$

where $V'_N(x)$ and $V'_C(x)$ are the potentials in the new variable. We can make a similar transformation for the model equation, viz;

$$s = e^Z,$$

$$R_L^0(s) = e^{Z/2} G_L^0(Z) \quad \dots(4.34)$$

to obtain the transformed model equation as

$$\frac{d^2 G_L^0(Z)}{dZ^2} + \frac{q_2(Z)}{\hbar^2} G_L^0(Z) = 0 \quad \dots(4.35)$$

where

$$\frac{1}{\hbar^2} q_2(Z) = e^{2Z} - 2ne^Z - \left(L + \frac{1}{2}\right)^2. \quad \dots(4.36)$$

We now apply the Miller-Good method to the set of equations (4.32) and (4.35). The phase shifts in the zeroth order can be expressed in terms of the original variables as

$$\sigma_L^0 = \sigma_L^c + \sigma_L^{\text{diff}} \quad \dots(4.37)$$

where

$$\sigma_L^c = A_{\text{reg}} \Gamma\left(L + 1 + i\eta\right), \quad \dots(4.38)$$

and

$$\begin{aligned} \sigma_L^{\text{diff}} = & \left(L + \frac{1}{2} \right) \left[\frac{\pi}{2} - \sin^{-1} \left(\frac{n\tilde{y} + \left(L + \frac{1}{2} \right)^2}{\tilde{y} \sqrt{n^2 + \left(L + \frac{1}{2} \right)^2}} \right) \right] \\ & + n \ln \left(\frac{\tilde{y} - n + \sqrt{\tilde{y}^2 - 2n\tilde{y} - \left(L + \frac{1}{2} \right)^2}}{\sqrt{n^2 + \left(L + \frac{1}{2} \right)^2}} \right) \\ & - \sqrt{\tilde{y}^2 - 2n\tilde{y} - \left(L + \frac{1}{2} \right)^2} + \int_{y_t}^{\tilde{y}} \sqrt{t_1(y)} dy \end{aligned} \quad \dots(4.39)$$

where y_t is the classical turning point, and \tilde{y} is a large value of y , which we choose. The choice is such that the total potential between the two nuclei is given very accurately by only the coulomb term $2n/\tilde{y}$.

One of the problems in working with a semi-classical method is to decide on the turning points that has to be taken into account in calculating the phase shifts. Here, we follow the prescriptions of Knoll and Schaeffer, who made a systematic analysis of this problem. For intermediate energies, there is a range of L values for which there are three real roots of $q_1(x) = 0$. We have shown in Fig. 4.1 the effective potential with the charge distribution (4.9). We have also shown in Fig. 4.2 and Fig. 4.3 a typical case for the C.M. energy $E_{\text{cm}} = 31.5$ Mev and for a potential given by (4.9) and (4.22). According to the criterion of Knoll and Schaeffer, for L values lower than the orbiting value

Fig. 4.1.

The effective potential $V_{\text{eff}}(r)$ which includes the real part of the nuclear potential, the centrifugal term and the coulomb field generated by GSM charge distribution, for different values of L .

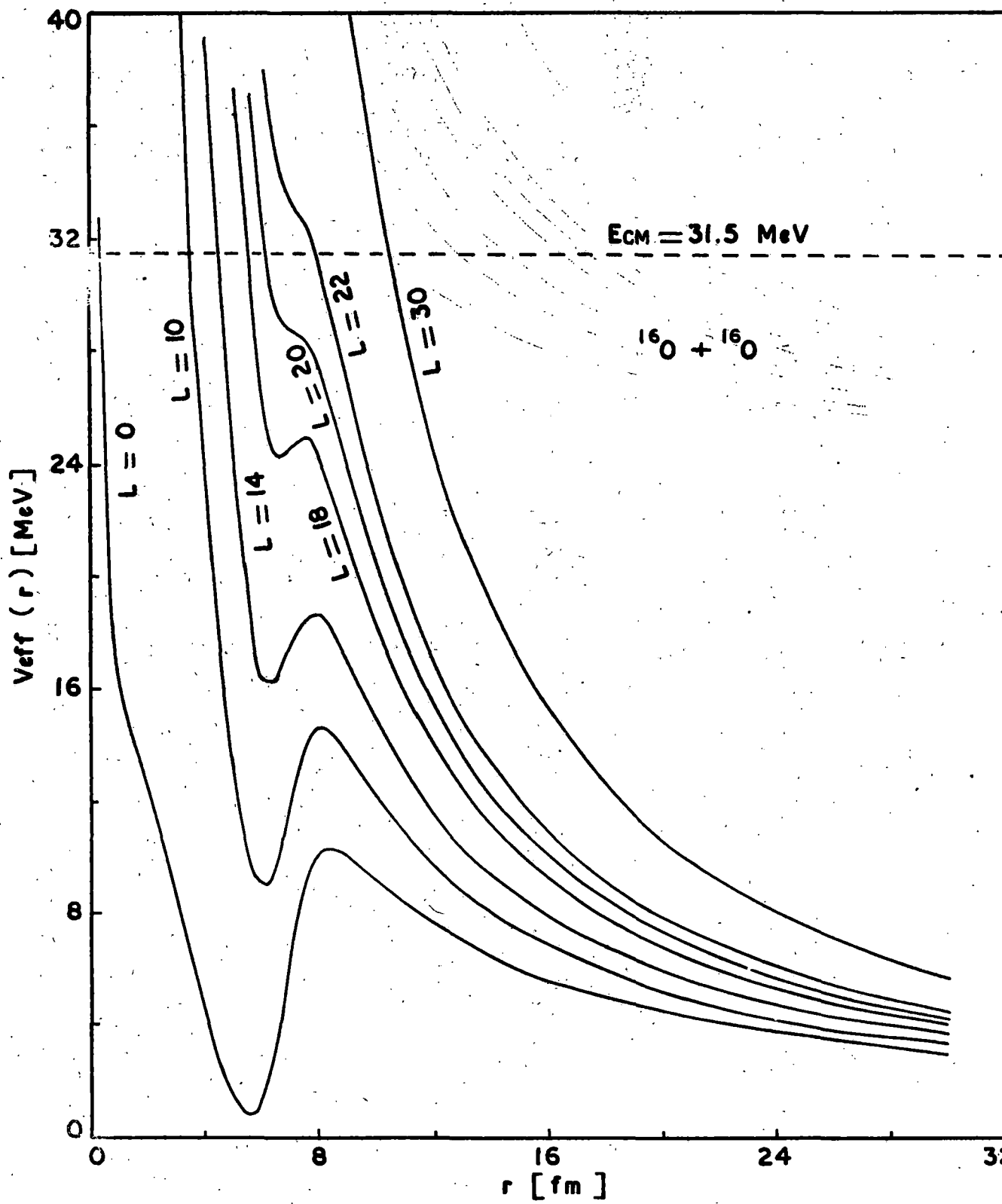


FIG. 4.1.

Fig. 4.2. The real function $t_1(y)$ for different values of L with GSM coulomb charge distribution at $E_{cm} = 31.5$ Mev.

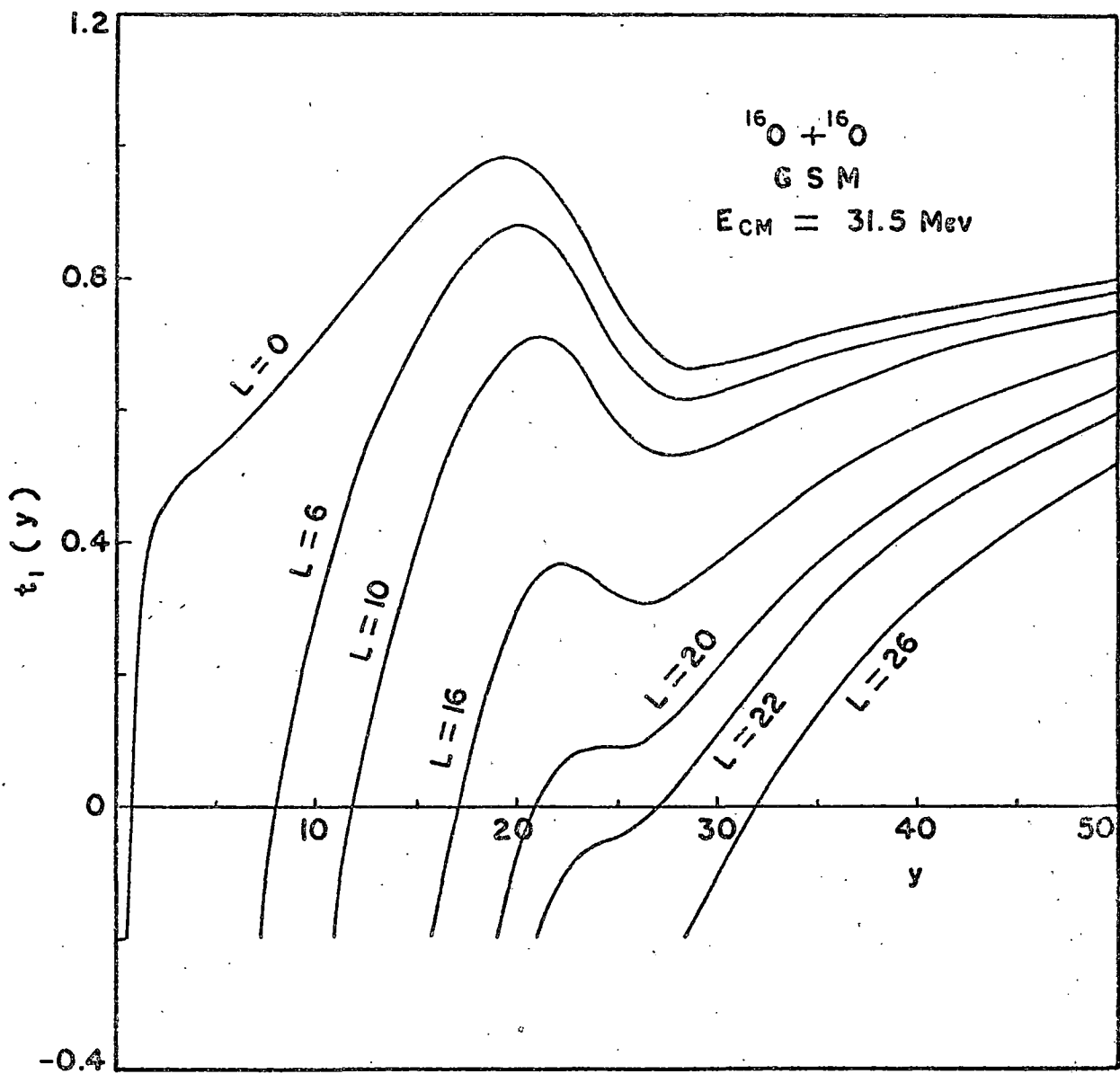


FIG.4.2 .

Fig. 4.3. The real function $t_1(y)$ for different values of L with uniform coulomb charge distribution at $E_{cm} = 31.5$ Mev.

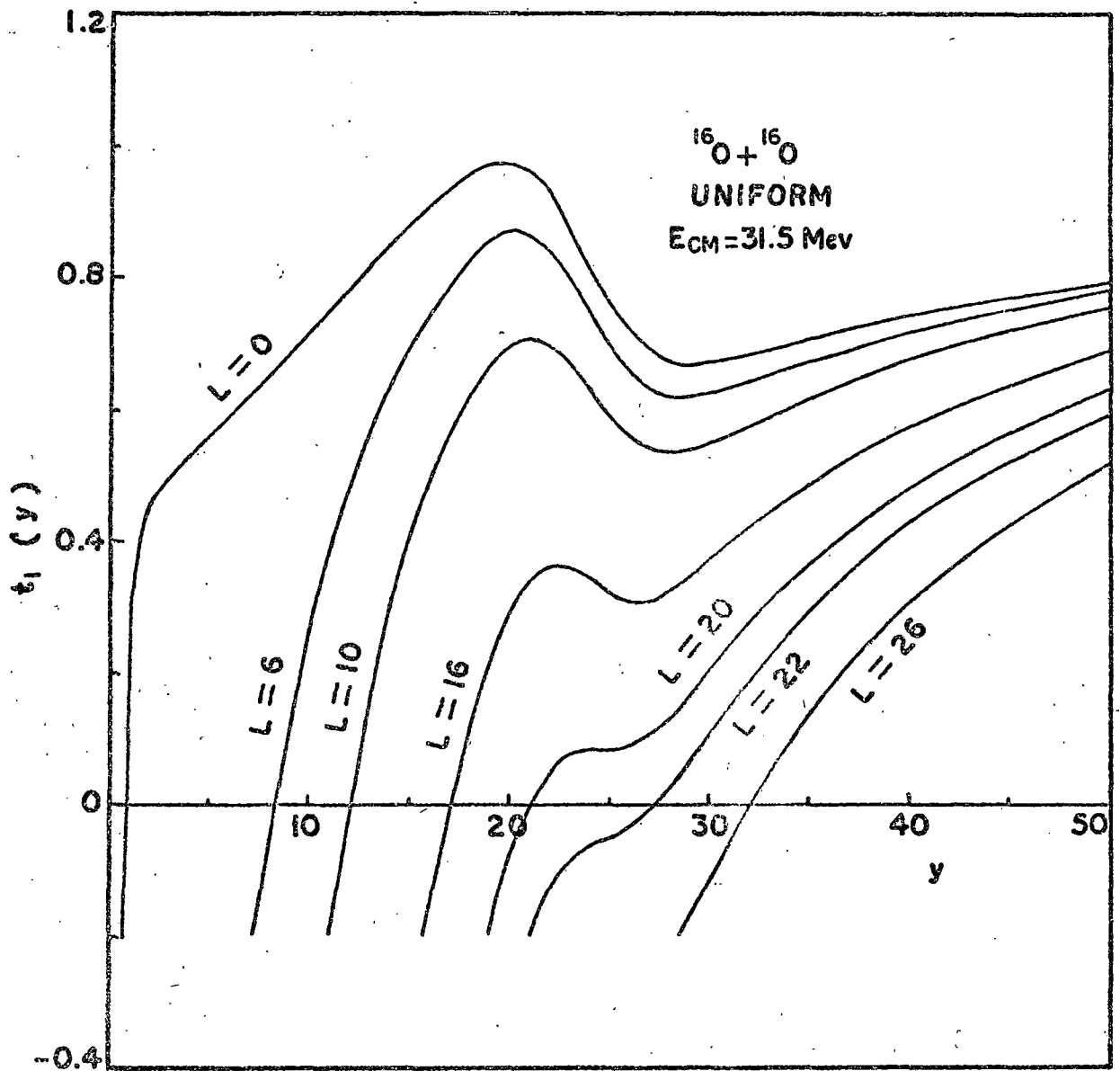


FIG. 4.3.

(when the maximum of the potential barrier equals E_{cm}), it is the inner turning point r_2 which contributes. At the orbiting value L_{orbit} , the phase shift jumps, since then the outer turning point r_1 alone starts giving the phase shift. At higher energies there is one real turning point which contributes. It may be pointed out that even for a real potential, one has complex turning points, which should, in principle, contribute for L values for which a pocket in the potential appears. Physically, this contribution accounts for the quantum mechanical reflection of the wave passing over a potential barrier. However, the effect of this term is small and we will not consider it in the calculation that follows. The problem of the choice of turning points for the complex trajectories is more involved and will be taken up in section.IV.5.

To calculate the cross-sections, one has to take into account the symmetry of the projectile and the target. Thus, one can write for the amplitudes,

$$\begin{aligned} \tilde{f}(\theta) &= f(\theta) + f(\pi - \theta) \\ &= \tilde{f}_M(\theta) + \frac{1}{ik} \sum_{L \text{ Even}} (2L+1) (e^{-2S(L)} e^{2i\delta_L} - e^{2i\delta_L^c}) P_L(\cos \theta) \end{aligned}$$

...(4.40)

where $S(L)$ is given by (4.25) and $\tilde{f}_M(\theta)$, the

symmetrized Mott scattering amplitude is given by

$$\begin{aligned}
 f_M(\theta) = & - \frac{n}{2K} \left[\frac{\cos \alpha}{\sin^2 \theta/2} + \frac{\cos \beta}{\cos^2 \theta/2} \right] \\
 & - i \frac{n}{2K} \left[\frac{\sin \alpha}{\sin^2 \theta/2} + \frac{\sin \beta}{\cos^2 \theta/2} \right]
 \end{aligned}
 \tag{4.41}$$

with

$$\alpha = 2 \delta_0^c - n \ln \sin^2 \frac{\theta}{2} , \tag{4.42}$$

$$\beta = 2 \delta_0^c - n \ln \cos^2 \frac{\theta}{2} , \tag{4.43}$$

and

$$\delta_0^c = \text{Arg} \Gamma(1 + in) . \tag{4.44}$$

The ratio σ_{el}/σ_M of the symmetrized scattering cross-sections can be easily calculated from the above relations. The summation in (4.40) can be terminated for a value of L so that all higher δ_L and δ_L^c differ by a quantity which is less than a preassigned small number.

IV.4. Results and discussions

We have calculated the phase shifts as well as the scattering cross-sections for the $^{16}_0 - ^{16}_0$ elastic scattering in the energy range $E_{cm} = 26.5 - 43.5$ Mev. The potential parameters were chosen as follows:

1. For the GSM charge distribution:

$$\alpha = 2, \quad a = 2.625 \text{ fm.}$$

2. For the uniform charge distribution:

$$R = 3.39 \text{ fm.}$$

3. The parameters for the nuclear potential were as follows⁴:

$$V_0 = 17 \text{ Mev,} \quad W_0 = 0.4 + 0.1 E_{cm}$$

$$R_0 = 6.8 \text{ fm,} \quad a_0 = 0.49 \text{ fm.}$$

The phase shifts were calculated explicitly upto $L = 100$, beyond which the phase shifts were assumed to be given by the coulomb phase shifts. Some of the real turning points for certain values of angular momenta are shown in Table VII. These turning points were used in evaluating the integral of equation (4.39). Our results are as follows:

- (a) Phase shifts and its variation with energy:

The calculated phase shifts show a smooth variation with energy. Some phase shifts with G S M charge

TABLE VII. Turning points (real) with G S M and uniform Coulomb charge distributions. The nuclear potential is real and as given in ref. 4.

L	Real turning points y_t	
	G S M	UNIFORM
0	0.724	0.704
2	3.499	3.416
4	5.955	5.856
6	8.118	8.038
8	10.075	10.026
10	11.895	11.876
12	13.628	13.633
14	15.314	15.333
16	16.996	17.020
18	18.751	18.776
20	20.876	20.897
22	27.190	27.191
24	29.866	29.866

distribution at different energies are shown in Fig. 4.4.

(b) Effect of the imaginary potential:

The effect of the imaginary potential is to supply a damping factor to each of the partial waves. In the present problem, ($E_{cm} = 31.5$ Mev) partial waves upto $L \sim 24$ are affected, the higher partial waves are not absorbed. The effect of this damping on the scattering cross-sections is shown in Tables VIII and IX.

(c) Effect of charge distribution:

The phase shifts for the G S M charge distribution and the uniform charge distribution show slight differences as shown in Table X, particularly for low values of L . For higher values of L ($L \sim 26$ and upwards) the difference almost vanishes, as expected. The results indicate that one will have to alter the radius of the uniform distribution appreciably, if one wants to fit the G S M results with a uniform model. This may be possible, since the scattering does not depend critically on the potential excepting in a certain region, mostly on the tail of the potential. But the consequent change of potential elsewhere may be reflected in the cross-sections for other processes, viz. fusion or transfer processes. It is, therefore, useful to consider the realistic G S M charge distribution in the study of heavy ion collision processes with nuclei like ^{16}O and ^{12}C .

Fig. 4.4. Variation of the semiclassical phase shifts with energy for elastic $^{16}\text{O} - ^{16}\text{O}$ scattering. The potential chosen is given by Maher et al.⁴

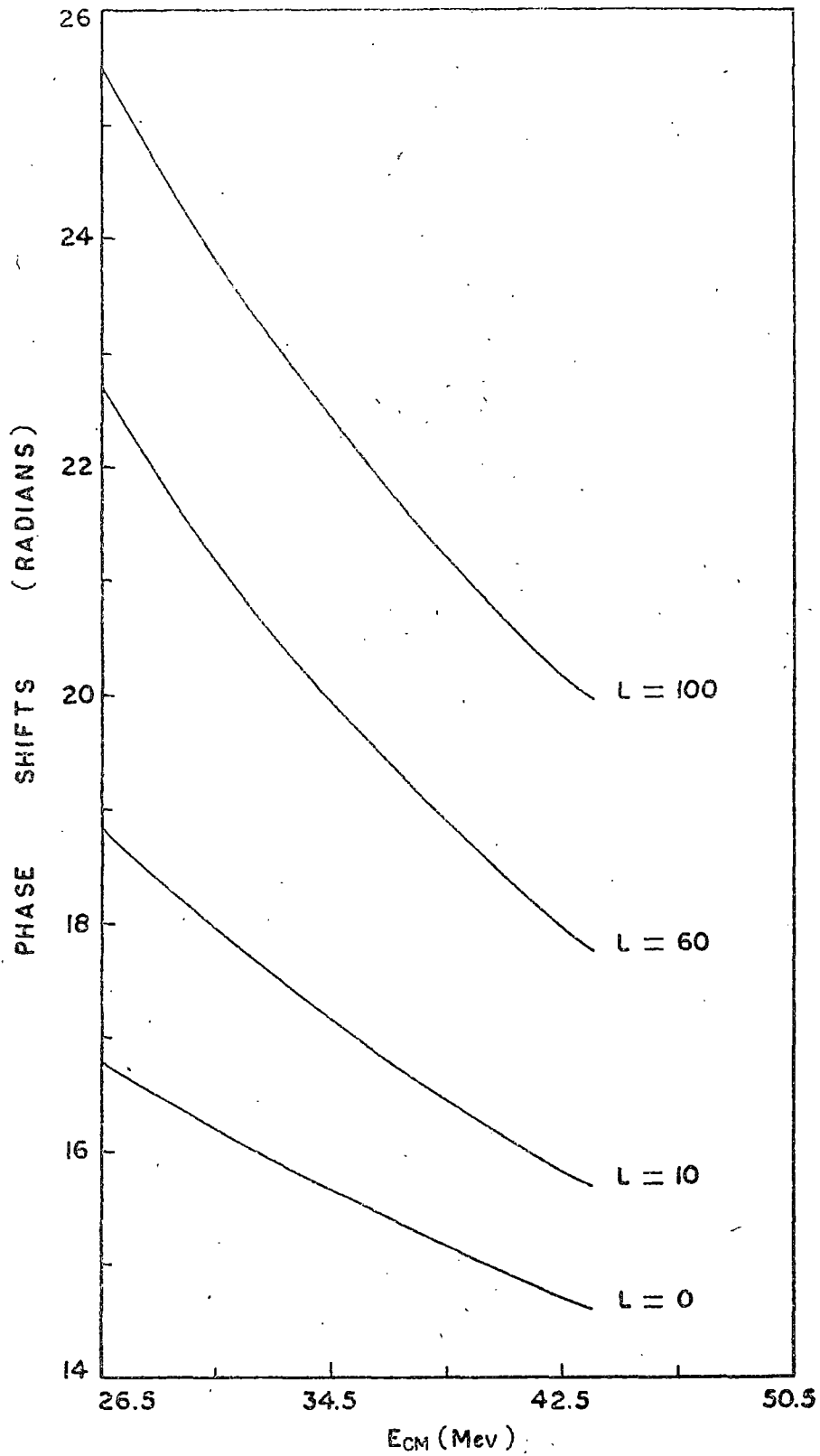


FIG. 4.4.

TABLE VIII. $^{16}\text{O} - ^{16}\text{O}$ elastic scattering
cross-sections with G S M coulomb
charge distribution.

θ_{cm} (degrees)	$d\sigma_{\text{el}}/d\sigma_{\text{MOTT}}$ (with $W_0 = 0.0$)	$d\sigma_{\text{el}}/d\sigma_{\text{MOTT}}$ (With $W_0 = 0.4 + 0.1 E_{\text{cm}}$)
20	0.241	0.241
25	0.193	0.196
30	0.999	0.992
35	0.023	0.022
40	0.912	0.925
45	0.426	0.424
50	0.328	0.320
55	0.494	0.499
60	0.087	0.091
65	0.901	0.890
70	0.643	0.648
75	2.588	2.632
80	0.793	0.784
85	0.049	0.047
90	0.464	0.469

TABLE IX. $^{16}_0 - ^{16}_0$ elastic scattering cross-sections with Uniform coulomb charge distribution.

θ_{cm} (degrees)	$d\sigma_{el}/d\sigma_{MOTT}$ (With $W_0 = 0.0$)	$d\sigma_{el}/d\sigma_{MOTT}$ (With $W_0 = 0.4 +$ $0.1 E_{cm}$)
20	0.223	0.224
24	0.466	0.471
28	0.310	0.307
32	0.839	0.834
36	0.036	0.037
40	0.873	0.883
44	0.204	0.208
48	0.848	0.841
52	0.063	0.060

TABLE X. The phase shifts for $^{16}\text{O} - ^{16}\text{O}$ elastic scattering with G S M and Uniform Coulomb charge distributions. The nuclear potential is given by a Woods-Saxon potential⁴.

L	Phase shifts (radians)	
	G S M	UNIFORM
0	16.051	16.195
2	16.244	16.366
4	16.605	16.687
6	17.018	17.060
8	17.409	17.421
10	17.736	17.728
12	17.968	17.950
14	18.078	18.057
16	18.029	18.011
18	17.760	17.746
20	17.114	17.106
22	16.110	16.200
24	16.358	16.358

IV.5. Complex Miller-Good Method

In this section, we shall consider the complex Miller-Good (CMG) method for studying the $^{16}\text{O} - ^{16}\text{O}$ elastic scattering phenomena. For simplicity, we shall consider energies for which there is only one contributing complex trajectory. This makes it necessary to consider an energy greater than 25 Mev in the C.M. frame. We have chosen the optical potential parameters given by Maher et al. It is known that this potential does not reproduce the experimental results, at the energies considered but our aim here is limited to the study of the efficacy of the CMG method in the case of a realistic scattering phenomenon. We have considered the scattering at $E_{\text{cm}} = 31.5$ Mev in detail and compared our results with (i) the results obtained by the perturbative method, discussed in the last section, (ii) the exact results and (iii) the experimental results. The last two results have been taken from Maher et al.

In applying the CMG method, the first step is to select the complex turning points which will make the dominant contribution. In the case considered, the complex turning point turns out to be the analytic continuation in the complex plane of the zeros of the function $\text{Re } t_1(y) = 0$, which are first calculated. We have shown in Fig. 4.5 the complex roots considered for calculating

Fig. 4.5.

Some complex turning points for different values of L for the $^{16}\text{O} - ^{16}\text{O}$ system at $E_{\text{cm}} = 31.5$ Mev with GSM coulomb charge distribution. The nuclear parameters are as in Ref. 4.

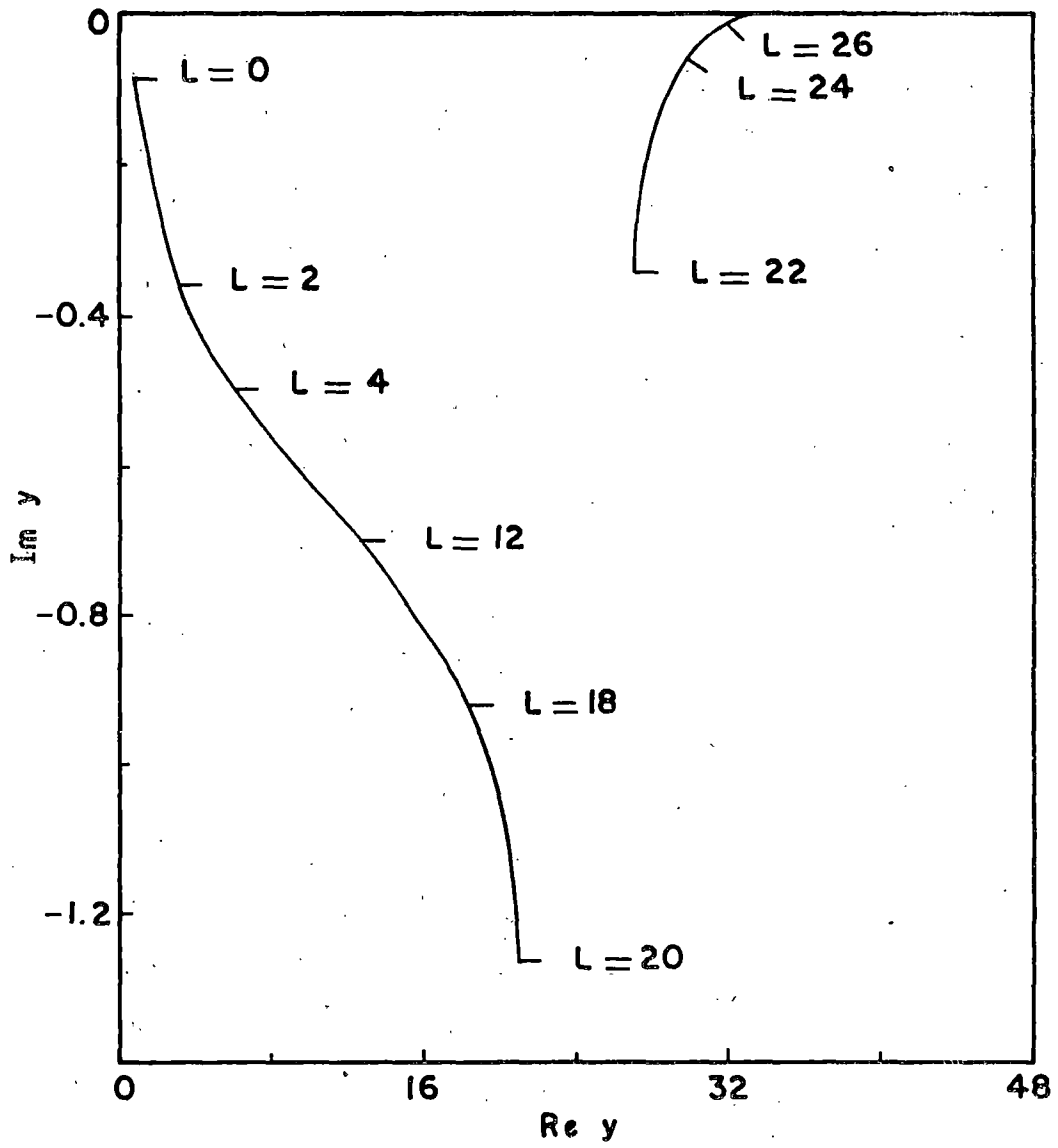


FIG. 4.5.

the phase shifts. These have been determined by an iterative method, giving the real root of $\text{Re } t_1(y)$ as an input. Our choice of the roots are consistent with the prescription of Knoll and Schaeffer. The path-integrations have been done along the contour shown in Fig. 2.1. The differential cross-section is calculated by considering (i) complex phase shifts upto $L = 20$, (ii) perturbative semiclassical phase shifts for $L = 22$ to $L = 100$, and (iii) coulomb phase shifts for larger L . The radial waves for $L = 22$ and higher are not much absorbed so that it is sufficient to consider complex integration upto $L = 20$.

We have shown the differential cross-section in Fig. 4.6 at $E_{\text{cm}} = 31.5$ Mev. The solid line gives the CMG results obtained as in above, while the dashed curve gives the results obtained by the perturbative method. The dotted line gives the experimental results of the Yale group⁴⁻⁶. The CMG results seem to give better agreement with the experimental results than the perturbative method, though the agreement is still poor. This is not surprising, because even the exact numerical calculation of Maher et al. shows poor agreement with the data (Fig. 4.7). The weakness of the potential is evident from the structure of the theoretical cross-section near 50° and 80° , which are out of phase with the experimental results. The approximate results obtained by us show almost the same features. However, the number and positions of the peaks

TABLE XI. Some complex turning points with GSM coulomb charge distribution for $^{16}_0 - ^{16}_0$ system at $E_{cm} = 31.5$ Mev. The nuclear potential is as given by Maher et al.

L	Real part	Imaginary part
0	0.7092	-0.0823
2	3.4478	-0.3548
4	5.9005	-0.5043
6	8.0682	-0.5808
8	10.0285	-0.6288
10	11.8501	-0.6683
12	13.5830	-0.7082
14	15.2664	-0.7544
16	16.9411	-0.8169
18	18.6761	-0.9276
20	20.6635	-1.2689
22	27.2648	-0.3408
24	29.8674	-0.0568
26	31.9916	-0.0160
28	34.0080	-5.0380 E-03
30	35.9950	-1.6309 E-03
32	37.9747	-5.3160 E-04
34	39.9537	-1.7329 E-04
36	41.9341	-5.6378 E-05
38	43.9161	-1.8299 E-05
40	45.8998	-5.9257 E-06

Fig. 4.6. Differential cross-section for $^{16}\text{O} - ^{16}\text{O}$ elastic scattering. The solid line represents the cross-section obtained by the CMG method and the dashed line by the perturbative treatment. The dotted line joins the data points of Ref. 4.

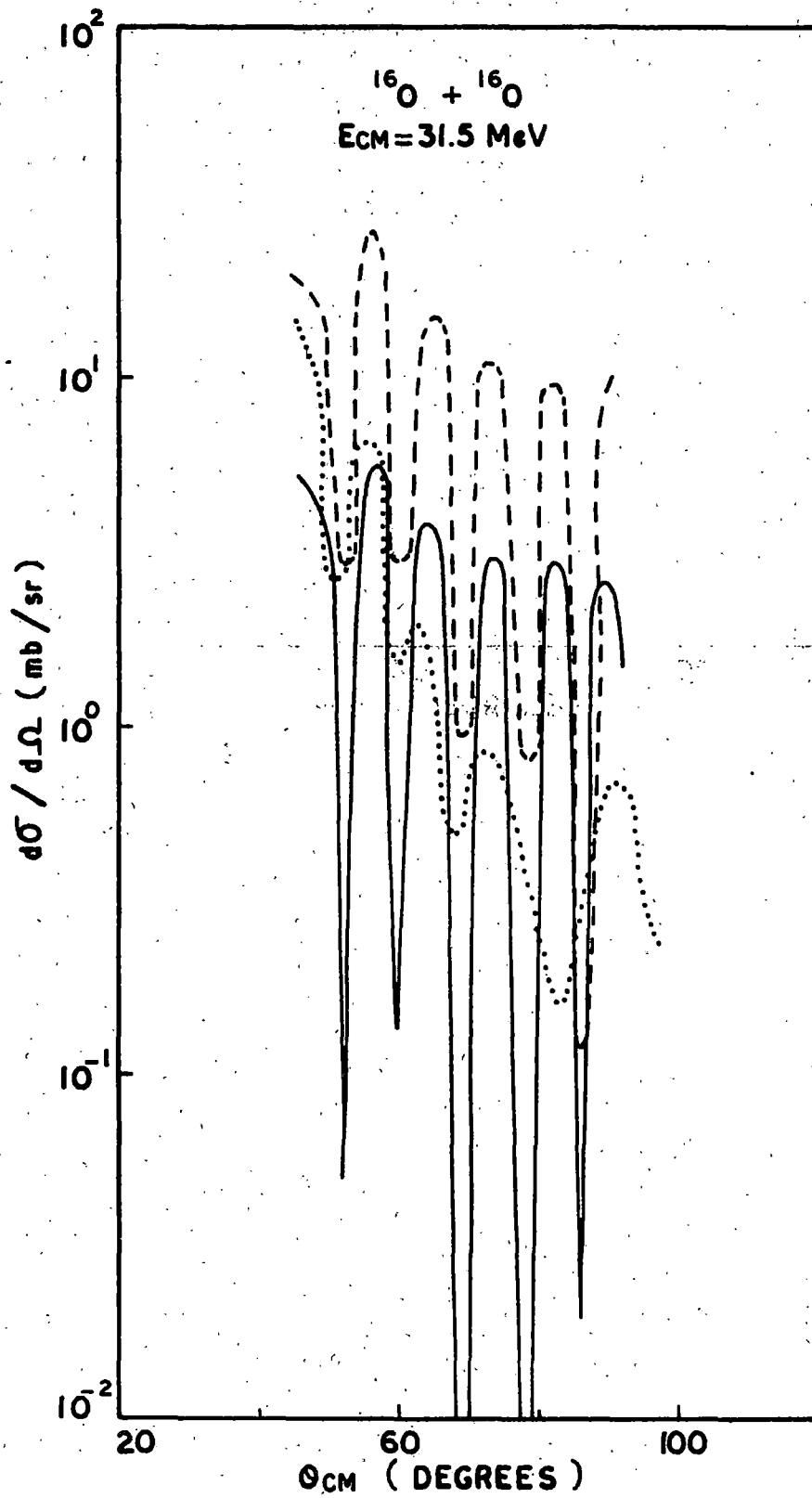


FIG. 4.6.

Fig. 4.7.

$^{16}_0 - ^{16}_0$ elastic scattering angular distributions reproduced from Ref. 4. The solid line gives the exact results and the dashed curve interpolates the experimental points.

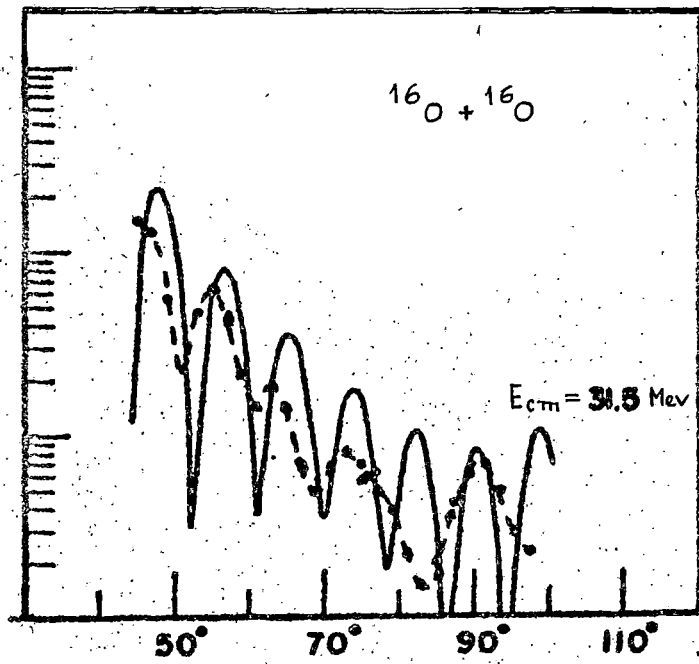


FIG. 4.7.

obtained by the approximate methods seem to agree well with the exact results, though there are still quantitative discrepancies, particularly near the minima, where correction terms of order \hbar^2 should have been considered.

It has been suggested that the shallow 17 Mev optical potential is not adequate and either a repulsive core and/or an ℓ -dependant potential is needed along with this shallow potential. Halbert et al⁷, following this suggestion, was able to get a better fit with the experimental results at higher energies. It is however, beyond the scope of the present work to aim for an accurate fitting of the potential. We would rather summarise our conclusions in the following:

The Complex Miller-Good method is an accurate method for determining the phase shifts, where the method is applicable in a simple way. However, the cases where the real part of $t_1(y)$ has three or more real zeros, the computation of the phase shifts becomes involved. Since in the semiclassical method, each radial equation has its own special feature and has to be studied separately, it is obviously not a good alternative to an exact numerical calculation. The semiclassical calculation, nevertheless, may serve a useful purpose, by giving an approximate estimate of the phase shifts and cross-sections⁸. The general feature revealed by these approximate calculations may be used as a guide for a subsequent numerical

computation. Moreover, where the gross features of the scattering are all that are needed to be known, the semiclassical method has already proved its utility. For scattering from simple potentials, the semiclassical methods often provide various bounds or exact results. Already in the realm of particle physics, the semiclassical approximations have found useful applications, particularly in the description of heavy quarkonia, the bound states of a quark and its antiquark. These states can be described in terms of a Schrödinger's equation, because at small distances the interaction potential which confines the quarks is small compared to the constituent quark masses. A number of useful bounds and exact results have been obtained here from semiclassical considerations? The heavy ion scattering processes are, of course, more complex in nature. Still, it is expected that the semiclassical methods, because of its basic simplicity, can be quite useful in studying at least the gross features of these complex manybody processes.

